Detectability of GRBs in CZT Imager of AstroSat

Rahul. G,[1]
[1] *1IUCAA Pune*

3 September 2022

ABSTRACT

Detection of GRBs using CZTI of AstroSat is reported regularly. Typically, about 325 GRBs per year are reported to be detected; out of these, CZTI detects about 75 per year. Here we present an analysis of all GRBs examined in the CZTI data and classified as detected and not detected (but visible) from 2015 October 1 to 2022 July 8. We define a detectability factor and examine its variation with GRB properties like fluence, T_{90}, E_{peak} and CZTI properties like the incident angle. We conclude that the detectability factor weakly depends on E_{peak} and incident angle. Further, CZTI is quite sensitive in the mid T_{90} (5 - 40 s) ranges. A careful re-examination of the data in different time scales and energy ranges may increase the number of GRBs detected by CZTI.

1 INTRODUCTION

CZTI data are regularly examined to identify GRBs. This is mainly done by a targeted search: looking at the data at the occurrence time of GRBs reported by other instruments. Data are also examined by a Machine Learning algorithm to look for new GRBs. There are a total of 2205 GRBs searched in the time interval of 2015 October 1 to 2022 July 8, and the search results are maintained at the CZTI POC in a Grand Catalogue. All pertinent information on the GRBs and the CZTI characteristics are stored in this catalogue.

In this work, we present the results of an analysis of this catalogue. It is found that out of the 2205 GRBs, 508 (23%) GRBs are earth occulted, 198 (9%) occurred when CZTI was in the SAA region (and hence not operational), 115 (5%) occurred when there was a gap in the data. Another dozen were ignored (weak detection or reason not specified). We note here that the fraction of GRBs not observed for these reasons (Earth occultation, SAA, data gap) are as per the expectations based on the relative times of these episodes.

Neglecting all this, we are left with 508 GRBs detected and 864 GRBs visible but not detected, which gives a total of 1372 GRBs. This translates into a detection rate of 37%: only 37% of all GRBs incident on CZTI when operating are detected. The overall geometric area of CZTI is about 1000 cm^2 (each for the CZT and the veto detectors), and in the operational energy range for all-sky monitoring (above 100 keV due to shielding and collimation), the effective area is close to 200 cm^2, comparable to Fermi GBM detectors. Hence, the lower detection rate of CZTI could be a combined effect of multiple factors like the dependence of sensitivity to the spectral hardness of GRBs and incident angle. Also, the detection algorithm may not be optimised for time and energy bins. To investigate these effects, we have selected 1044 GRBs with measured values of T_{90} and fluence for our further analysis.

2 FLUENCE VS T90

A Fluence Vs T_{90} plot is made using the data of 1044 GRBs (Fig.1). The detected GRBs are shown in orange and visible (but not detected) GRBs in blue. Most of the GRBs are detections from Fermi GBM. The size of the circle in the figure is proportional to the logarithm of E_{peak}. An 'x' mark indicates that the E_{peak} value is unavailable for that GRB. From the figure, we cannot discern any significant dependence of the detectability based on E_{peak} (we have tried to quantify this observation, see later). It can be seen from Fig.1 that there is a somewhat sharp cutoff of the GRBs in the fluence – T_{90} plane indicating that Fermi GBM is a truly wideband all-sky monitor and hence fluence and T90 uniquely dictate its sensitivity. CZTI detection, on the other hand, does not show such a sharp boundary. We can see that CZTI is relatively less sensitive for short GRBs but reasonably sensitive in the T_{90} range of 5 – 40 s. Even in this time range, there are several GRBs with fluence an order of magnitude higher than the visible sensitivity limit but are not detected by CZTI.

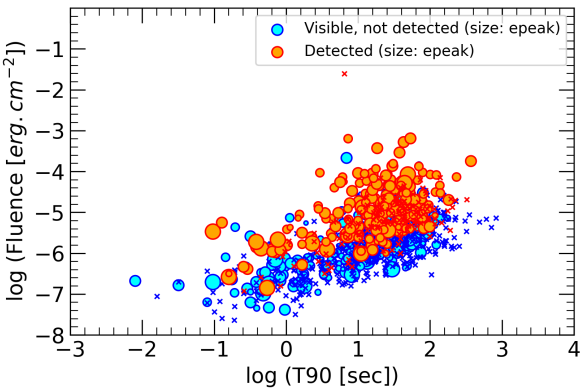

Figure 1. A plot of Fluence Vs T_{90} for 1044 GRBs, with GRBs detected by CZI in orange and GRBs visible to CZTI but not detected in blue. The size of the circle is proportional to the logarithm of the E_{peak}. The cross mark indicates that the E_{peak} values are unavailable for that specific GRB.

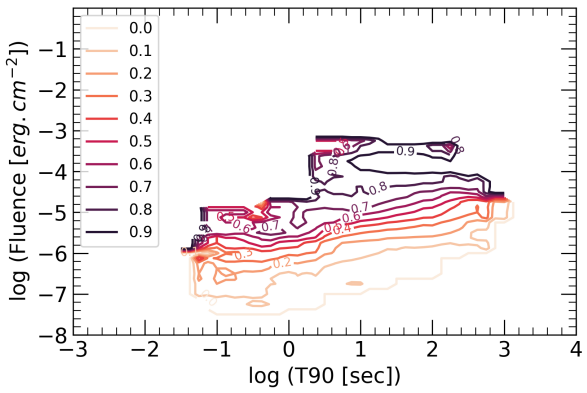

Figure 2. A contour plot of the detectability factor (δ) of GRBs in CZTI, defined as the ratio of detected GRBs to the total incident GRBs. δ is estimated in equal cells of dimension 0.5 dex × 0.5 dex. A sliding window technique is used to get a smooth contour. The δ values are noted inline on the plot.

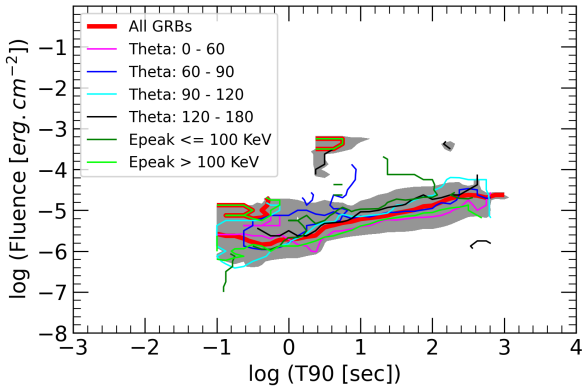

Figure 3. This plot shows the comparison of the detectability factor δ for different incident angles (Theta) and E_{peak}. The thick red line is the δ = 0.50 (50% sensitivity) line for all GRBs. The other lines represent 50% sensitivity for respective theta and E_{peak} ranges (mentioned in the plot). The shaded region indicates the region between the 0.25 and 0.75 contour lines for all GRBs. It can be seen that the shaded region is much wider than the range of contours for the other parameters.

3 DETECTABILITY FACTOR (δ)

We define a detectability factor (δ) as the ratio between the number of detected GRBs in a cell (in the Fluence – T_{90} space) and the total incident GRBs in that cell. A sliding window method is implemented to create a smooth contour plot (Fig.2). The δ = 0 means 0% sensitivity, δ = 1 means 100% sensitivity and all values in between them lies in corresponding sensitivity. We can see a smooth transition from δ = 0 to δ = 1.

Two further analyses are done to investigate any significant shifts in the sensitivity based on the other parameters like the incident angle (theta) and E_{peak}. The GRBs are categorized as (a) GRBs in different theta ranges and (b) GRBs that have Epeak above 100 keV and below 100 keV. The results are shown in Fig.3. The δ = 0.5 line for all GRB is shown in red, and a confidence band between 0.25 to 0.75 is shown as a shaded region in the plot. The δ = 0.5 lines for different theta ranges are drawn in the same plot. A similar analysis is done for GRBs with E_{peak} above and below 100 keV (Fig.3).

E_{peak} (KeV)	Theta range (deg)	No. of GRBs	rms error	Intercept
-	All (0 - 180)	313	0.505	8.319
-	0 - 60	107	0.334	8.484
-	60 - 90	70	0.436	8.451
-	90 - 120	69	0.602	8.124
-	120 - 180	67	0.544	8.115
≤ 250	-	95	0.389	8.282
> 250	-	101	0.473	8.272

Table 1. Result of fits to the Fluence vs total counts (detected in CZTI) plots (linear fit in the log space with slope kept fixed at 1). Intercept and rms error for GRBs in different theta and E_{peak} ranges are shown, along with the results for all GRBs.

The 0.5 line for GRBs below 60 degrees is lower than that for the overall GRBs, and the 0.5 line for GRBs above 60 degrees is above the line for all GRBs. There is a noticeable shift in the sensitivity line for GRBs with E_{peak} above 100 keV and below 100 keV. But, looking at the overall trend, these shifts may not be significant enough to explain the full range of δ seen for all GRBs. We attempt to quantify this by examining the total detected counts in CZTI.

4 FLUENCE VS TOTAL COUNTS

The total counts from CZTI detection are used for this analysis. The GRBs are categorized into different theta ranges, and the result is linear-fitted with a slope fixed as 1. The shift in intercept and RMS error is noted down in Table.1.

From Table 1, when we look at theta ranges 0 - 60, 60 - 90, 90 - 120, and 120 - 180, the intercept is 8.480, 8.440, 8.124, and 8.121 respectively. This lies in the expected decrease in sensitivity for these angles because the effective area between angles 0 and 60 degrees is twice that of the region between angles 60 and 180 degrees.

5 CONCLUSION

From the above analysis, we can say that theta dependence is not the only reason for not detecting at lower fluence. Further study is required to pinpoint the exact sensitivity of CZT Imager.

REFERENCES

FERMI GRB Catalogue,
Link: https://heasarc.gsfc.nasa.gov/W3Browse/fermi/fermigbrst.html

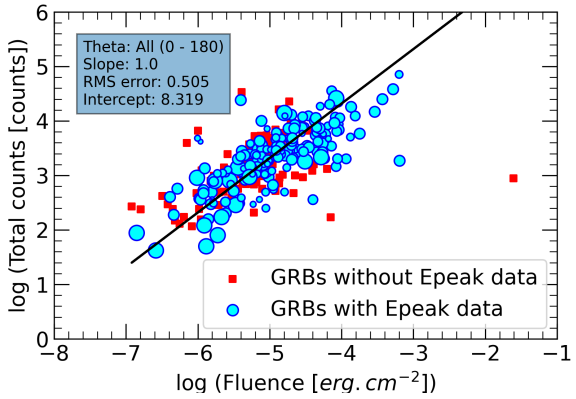

Figure 4. A plot of fluence Vs the total counts detected in CZTI. GRBs with available E_{peak} are shown in blue, with the size of the circle proportional to the log of E_{peak}. The straight black line is the linear fit with the slope kept as 1 for all GRBs.